International Journal of Bioprinting

ORIGINAL ARTICLE

Using Large-Scale Additive Manufacturing (LSAM) as a Bridge Manufacturing Process in Response to Shortages in PPE During the COVID-19 Outbreak

Elizabeth G. Bishop and Simon J. Leigh

School of Engineering, University of Warwick, Coventry, CV4 7AL, UK

Abstract: The global COVID-19 pandemic has led to an international shortage of personal protective equipment (PPE), with traditional supply chains unable to cope with the significant demand leading to critical shortfalls. A number of open and crowd-sourcing initiatives have sought to address this shortfall by producing equipment such as protective face shields using additive manufacturing techniques such as fused filament fabrication (FFF). This paper reports the process of designing and manufacturing protective face shields using large-scale additive manufacturing (LSAM) to produce the major thermoplastic components of the face shield. LSAM offers significant advantages over other additive manufacturing technologies in bridge manufacturing scenarios as a true transition between prototypes and mass production techniques such as injection moulding. In the context of production of COVID-19 face shields, the ability to produce the optimised components in under five minutes compared to what would typically take one to two hours using another additive manufacturing technologies meant that significant production volume could be achieved rapidly with minimal staffing.

Keywords: Additive Manufacturing, 3D Printing, COVID-19, Coronavirus, Face Shield, PPE

Corresponding Author:
Elizabeth G Bishop,
School of Engineering, University of Warwick,
Coventry, CV4 7AL, United Kingdom;
Email: E.G.Bishop@warwick.ac.uk

Article Information

Received: May 14, 2020
Accepted: June 15, 2020

(This article belongs to the Special Section: Research and Applications of 3D Printing and Bioprinting for Covid-19)

1.0 Introduction

In December of 2019, an outbreak of infections from a novel coronavirus (now named SARS-Cov-2) was reported in China [1]. The class of viruses known as coronaviruses are responsible for most of the common colds and have often arisen due to transmission from animals to humans [2]. Initially focussed on Wuhan in the Hubei province, [3] the infection has since spread globally, with the spread of coronavirus disease 2019 (also more commonly known as COVID-19) reaching the necessary level of spreading to be classified as a global pandemic according to the World Health Organisation (WHO) [4]. At the time of writing, it is believed that over 4 million people have been infected globally, leading to over 278,000 deaths [5]. It has been established that the contagiousness of the disease is higher than previous outbreaks such as SARS in 2002-2004 [6] and can be transmitted through airborne droplet and contact transmission [7]. It has also been established that people are able to transmit the infection despite not obviously displaying symptoms (asymptomatic) [8].

For these reasons, the wearing of personal protective equipment (PPE) has become a vital requirement for frontline medical staff, those with critical caring responsibilities and key workers facing increased potential exposure to SARS-Cov-2. The WHO has recommended that PPE also includes eye protection to safeguard against droplet and airborne transmission [9]. Droplet transmission (as happens with influenza) occurs when droplets from an infected individual that are generated during coughing, sneezing or even talking pass through the air, and land on the eyes, nose and mouth of another individual leading to infection [10].

With this increased global demand for PPE, governments and organizations have struggled to source enough for millions of regular PPE users, let alone for non-typical users such as pharmacies and general practitioners who are now at increased risk of infection during their daily activities. These supply chain issues have arisen due to a global shortage of PPE items such as eye protection/face shields and the inability to manufacture enough items quick enough [11]. In response to this unprecedented demand, many companies, academic institutions and individuals have sought to use democratised manufacturing facilities and equipment such as 3D printers (generally FFF, fused filament fabrication systems) to produce components for much needed PPE items such as face shields [12, 13]. This manufacturing effort has seen members of the international 3D printing community come together in vast, rapidly formed collaborative networks to address the PPE shortfall in a way reminiscent of the often-proposed concept of localised microfactories [14, 15]. In the context of a traditional product development cycle, this type of activity can be likened to bridge manufacturing, where the use of additive manufacturing techniques is used to bridge the gap between small volume, time-intensive manufacturing processes and other mass manufacturing techniques such as injection moulding when increased demand makes the production of tooling and moulds a cost-effective option.

Due to the prevalence of desktop FFF 3D printers, most of the designs being manufactured by these global communities are optimised for common 3D printer formats, such as build plates of approximately 200 × 200 mm and 0.4 mm (*sub mm*) extrusion nozzles [16]. These limitations generally mean that the main components of face shields can take one to two hours to produce, which presents a significant issue for producing larger volumes of components. Typical thermoplastic deposition rates on desktop 3D printers are usually on the order of 10 mm^3/s [17]. LSAM systems have build volumes with dimensions of 1 m or greater and typically use nozzles with diameters of 1 mm or greater, allowing for significantly higher deposition rates on the order of 100 mm^3/s. LSAM has been used previously to manufacture tooling for various applications [18-20], as well as being used for direct manufacture of large single objects [21] such as furniture [22] and bike frames [23].

The ability to deposit thermoplastic materials at rates of up to 100 mm^3/s with LSAM means that bridge manufacturing rates for PPE components can be significantly increased addressing immediate requirements in advance of an eventual increase in production capacity using techniques such as injection moulding. In this paper, we report the design and development of face shield components optimised for production using LSAM technology, such that a component that would normally take one to two hours to produce can be made in under five minutes. The development of process parameters to ensure continued part quality with larger part volumes per production run is also presented.

2.0 Materials and Methods

The headbands were printed on a 3D Platform 300 Series Workbench Pro (3D Platform, USA) with HFE 300 3D Printer Extruder, fitted with a 1.8 mm nozzle. The material used for the thermoplastic component was 3DFilaPrint Premium PLA 2.85 mm (3DFilaPrint, UK). All print parameters were previously determined empirically through an iterative process. The key print parameters used were: 1.8 mm extrusion width; 1 mm layer height; 0% infill; 230°C extrusion temperature; 50 mm/s default printing speed.

3.0 Results and Discussion

A typical face shield for use during the COVID-19 pandemic comprises of several key components (Figure 1): a headband (**1**), clear lens/visor (**2**), a strap (**3**), top protection (**4**) and a bottom support piece (**5**). Other crowdsourcing projects have sought to produce the headband and bottom support pieces using desktop 3D printers. Within this study, LSAM was applied in the same way but with the goal of speeding up production of these parts by approximately 20×.

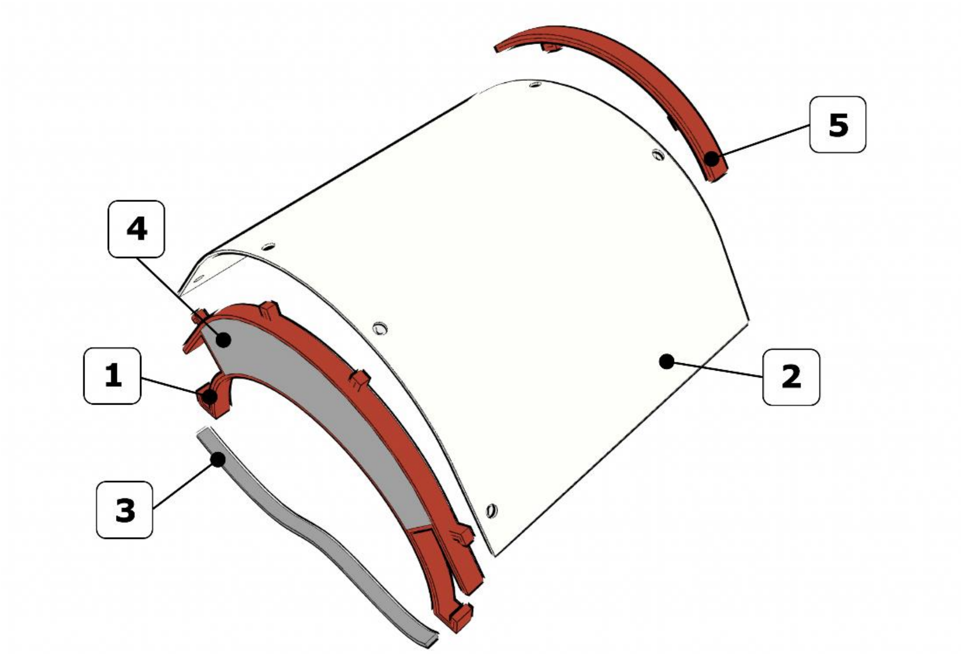

Figure 1: Typical components that make up an emergency face shield.

The design requirements dictated by the functionality of the 3D printed parts were as follows (*key function analysis, Figure 2*). The headband is needed to easily conform to the user's head and hold a lens/visor with sufficient splash protection to meet the required regulations. The headband also needed to have a way to be held onto the head of the user using some form of strap and be lightweight as it would need to be worn for extended periods of time. The parts of the face shield should also be entirely free from sharp regions or defects that are likely to cause injury or discomfort to a user. To aid clarity for this paper, the production of the largest component, the headband will be the focus. As the target production time for the headband was sub-10 minutes, the design needed to be fully optimised for production with LSAM, leveraging the key advantages of the process. The material used for the thermoplastic component was 3DFilaPrint Premium PLA 2.85 mm (3DFilaPrint, UK).

In order to optimise the design, the obvious strategy to adopt first in designing a part for LSAM is reducing the amount of material required (*dematerialisation*) which dictates that all material must contribute to the critical function of the device, with no excess, unrequired material present.

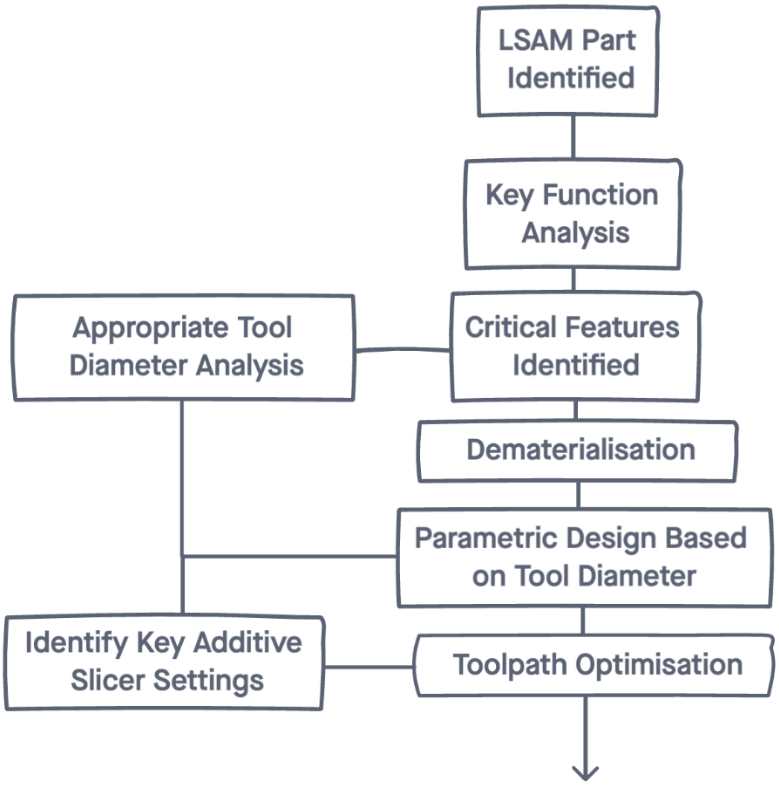

Figure 2: InVision Freehand schematic showing the design methodology employed in optimising a design for LSAM.

In order to print effectively, the minimum feature size of the printed design needs to be specifically selected as it is determined by the nozzle diameter of the LSAM system (*tool diameter analysis*). For example, the minimum horizontal width of any section which protrudes from the main headband must be at least 2× nozzle diameter, but no larger than 2.5× nozzle diameter, or else, the printed extrusions will not bond together (*parametric design based on tool diameter*). To reduce overall travel moves made by the printer, the largest possible nozzle should be chosen, but to ensure that the parts stay lightweight with sensible feature sizes, a balance must be struck. In this case, a 1.8-mm nozzle was selected to achieve this required balance. The 1.8-mm nozzle allowed for deposition rates of 92 mm^3/s, (printing a headband with less than 20 g of PLA) whilst allowing for the features to be small enough for functions such as the attachment of the lens/visor. The headbands were designed with no overhanging sections to ensure that no material or time was wasted in printing support material. The final strategy to adopt is to ensure that every move of the print nozzle in the print job is a useful move, i.e. all moves made are contributing to the deposition of material and there are minimal non-print travel moves (*toolpath optimisation*). In order to ensure this toolpath optimisation, the design was first optimised for production with only single walls (Version 1) and then optimised for production using 'vase mode' (Version 2). In vase mode (also known as *'spiralise outer contour'*) throughout the print, the nozzle does not (i) travel without printing, (ii) retract, or (iii) stop extruding.

3.1 Initial design (Version 1)

The initial design took inspiration from various community-driven face shield designs available (e.g. *N3DPS* [24], *Prusa* [25], *Verkstan* [26]*)* and the digital design work was carried out in Autodesk Fusion 360. A key focus for the design was to ensure the final shield would pass any relevant regulatory testing, which determined aspects such as the height of the headband being no less than 10 mm tall. The second key design aspect was the attachment points for the clear lens/visor. The visor holes would be made using a standard 6-mm diameter hole punch and therefore, the attachment points were designed with a 5.5-mm width, distributed around the front loop of the headband. Ensuring that the printed parts were not sharp and likely to injure the user might normally require filleting of edges in the design, but fillets were not required in the CAD model (Figure 3a) as when printing with LSAM, the machine will essentially 'self-fillet' at sharp turns which can be seen in comparing the corners of the strap attachment points in Figure 3a and Figure 3c. The final design focus was on ensuring the individual sections of the headband met the requirements based on a tool diameter of 1.8 mm (*parametric design based on tool diameter*). Therefore, the front and rear sections were set to 1.8-mm thick, and the thicker sections of the design set to double the extrusion width (3.6 mm), crucially with a 0.1 mm gap between the deposited tracks to allow for single wall extrusion printing to happen rather than the slicer infilling the region, which can been seen in the sliced file in Figure 3b. An example of final print can be seen in Figure 3c. The preparation of the designs for printing was carried out in Simplify3D and printing was carried out using a 3D Platform Workbench system. This version of the design took just 5 minutes to print. The nature of the printing method meant that the seam line (from the start and stop point of the layers) led to defects in the final print (as can be seen on the strap attachment point) meaning some hand finishing was required.

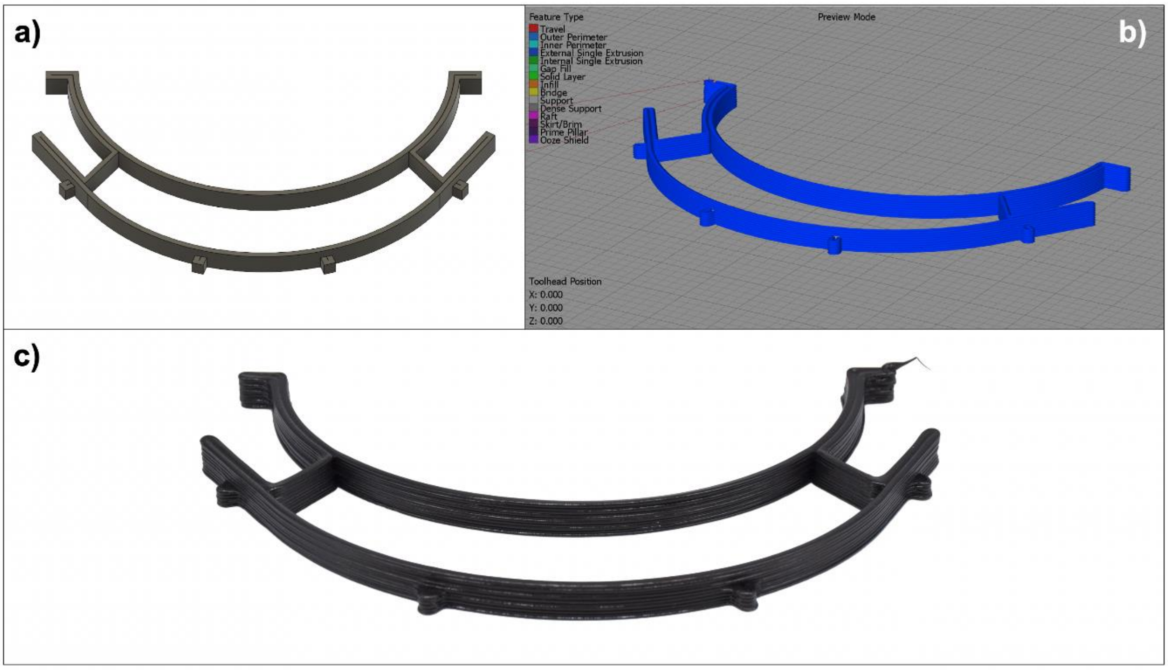

Figure 3: Initial design for face shield components produced using LSAM, a) showing the CAD model, b) the Simplify3D sliced print preview and c) the final printed part.

3.2 Design iteration (Version 2)

Whilst the initial design worked, the clear lens/visor which is held on at 4 points, did not hold on very well, as the lip which can be found in many of the small scale designs needed to be removed for LSAM to be possible. The headband was therefore redesigned to change the two outer two attachment pins into hooks which could be printed with the 1.8-mm nozzle which vastly improved the design. At this point, it was also decided to change the design to allow for 'vase mode' to be employed (*toolpath optimisation*) Vase mode is where the printhead moves continuously in Z throughout the print, varying the Z parameter slightly, in contrast to printing a single layer, at constant Z value, stopping in XY and then moving to the next layer. The toolpath for a 'vase mode' print is generated via the additive slicer used for LSAM, by taking a solid and extracting the outermost perimeters. Thus, the headband design was modified to create a fully solid design (Figure 4a), with the slicer software generating the required toolpath (Figure 4b). The resulting headband was printed in 4 minutes. The most notable impact of using this strategy is that the visible seam line and defects are completely removed, thereby removing the requirement for any hand finishing (Figure 4c).

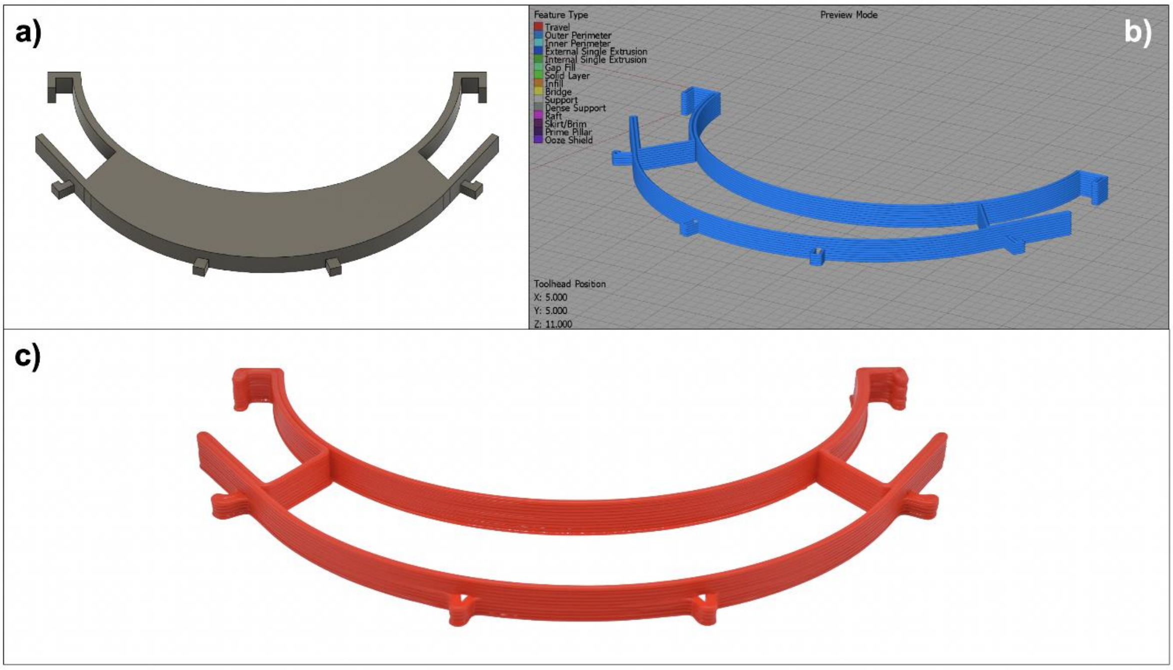

Figure 4: Improved face shield design using LSAM, a) showing the CAD model, b) the Simplify3D sliced print preview and c) the final printed part.

3.3 Speeding up the manufacturing process / sequential deposition for quality

In order to speed up the manufacturing process and ensure continued part quality (crucial for scaling up production), the use of a sequential manufacturing strategy was employed. In a conventional additive manufacturing process, when producing multiple parts on a single print bed, all the parts will be produced in parallel such that the layers of each are incremented at the same time. Producing parts in this way leads to lots of non-print travel moves (red lines) as can be seen in the toolpath preview in Figure 5a. Printing multiple parts on a single print bed using traditional parallel printing with FFF systems can result in defects on the parts, such as stringing that can occur when material exits the nozzle during non-print moves between parts [27, 28]. Stringing is often difficult to minimise, especially when using large print nozzles. When producing multiple copies of the face shield parts on a single print bed it was found that stringing often occurred (Figure 5b), leading to significant, sharp defects and random deposits of material on certain regions of the headband piece (Figure 5c). This parallel print strategy also meant that ‘vase mode’ could not be used, leading to reintroduction of the seam line defects caused by the layer change. The total print time for 27 headbands was 2 hrs 9 min giving a time of 4 min 47 s per headband.

Instead, a sequential production process was employed, where each part was first completed, in ‘vase mode’, before a new part was commenced (Figure 5d), significantly reducing the number of travel moves (red lines) during the total print. The small overall Z height of the individual parts ensured that the sequential deposition was achievable by limiting potential print head collisions with parts already produced. Switching to sequential deposition had no significant impact on part production time and improved the quality of the final parts, with no visible defects or sharp areas requiring hand finishing (Figure 5b and 5c). Interestingly, switching to sequential deposition (whilst less could be printed on the bed at the same time due to print head geometry constraints), actually reduced the print time per headband (compared to parallel printing) as time is saved in removing the travel moves within a single layer. Other benefits of using sequential printing include minimising both the risk of a single print failure causing a whole print bed of parts to be damaged and the risk of the print material running out and leaving a whole print bed of incomplete parts. The resultant print time for a headband was 3 min 20 secs per headband (1 hr 30 min for 27 headbands).

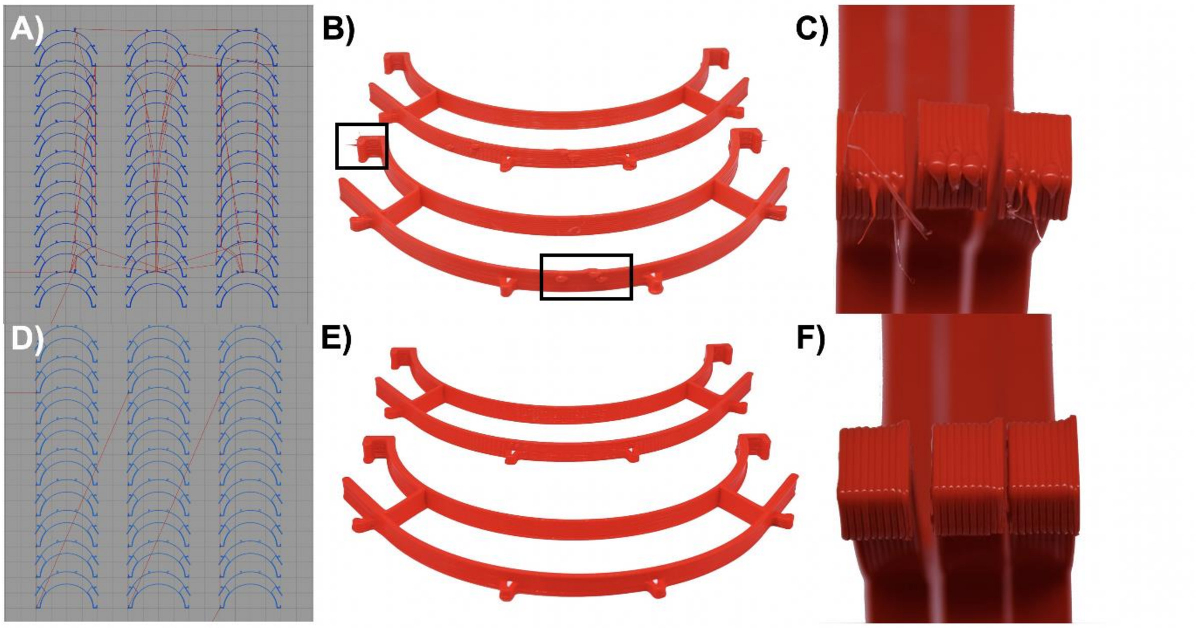

Figure 5: a) Toolpath preview of parallel print process with travel moves shown in red, and photos showing comparison of the quality of b) multiple parts on a single build plate using parallel production strategy with defect areas highlighted and c) multiple defects versus d) toolpath preview of a sequential print process and photos of b) multiple parts on a single build plate using sequential production strategy showing d) minimal defects.

Overall, the production time achieved was significantly less compared to other community and open-source face shield designs. In order to quantify the reduction in time, multiple other designs were produced on either a standard desktop 3D printer (Ultimaker 3) and the 3D Platform with the results shown in Table 1.

Table 1: Results showing different print times for open source and the headbands described in this paper.

Design	N3DPS [24]	Prusa-reduced [25]	Verkstan [26]	Version 2 (Desktop Printer)	Version 1	Version 2	Version 2 Parallel	Version 2 Sequential
Printer	Ultimaker 3	Ultimaker 3	Ultimaker 3	Ultimaker 3	3DP	3DP	3DP	3DP
Nozzle Size (mm)	0.4	0.4	0.4	0.4	1.8	1.8	1.8	1.8
Layer Height (mm)	0.2	0.2	0.2	0.2	1	1	1	1
Total Print Time (min)	115	75	69	92	5	4	129	90
Print Time per Headband (min)	115	75	69	92	5	4	4 min 47 s	3 min 20 s

3.4 Mechanical Testing

In order to further compare the different designs and ascertain their robustness, the *Version 2* printed on the large-scale system (3DP) and the *Version 2* printed on a desktop system (Ultimaker) were mechanically tested (*tensile parallel to layers*) alongside other open source designs, with the results shown in Figure 6. Version 2 (Desktop) had a similar breaking force to the Prusa-r design, the Verstan and N3DPS show a different characteristic plot which reflects the very different design approach to these two designs. Version 2 (Large-Scale) can be seen to be much stronger with a breaking force of 1120 N compared to the Version 2 (Desktop) of 320 N.

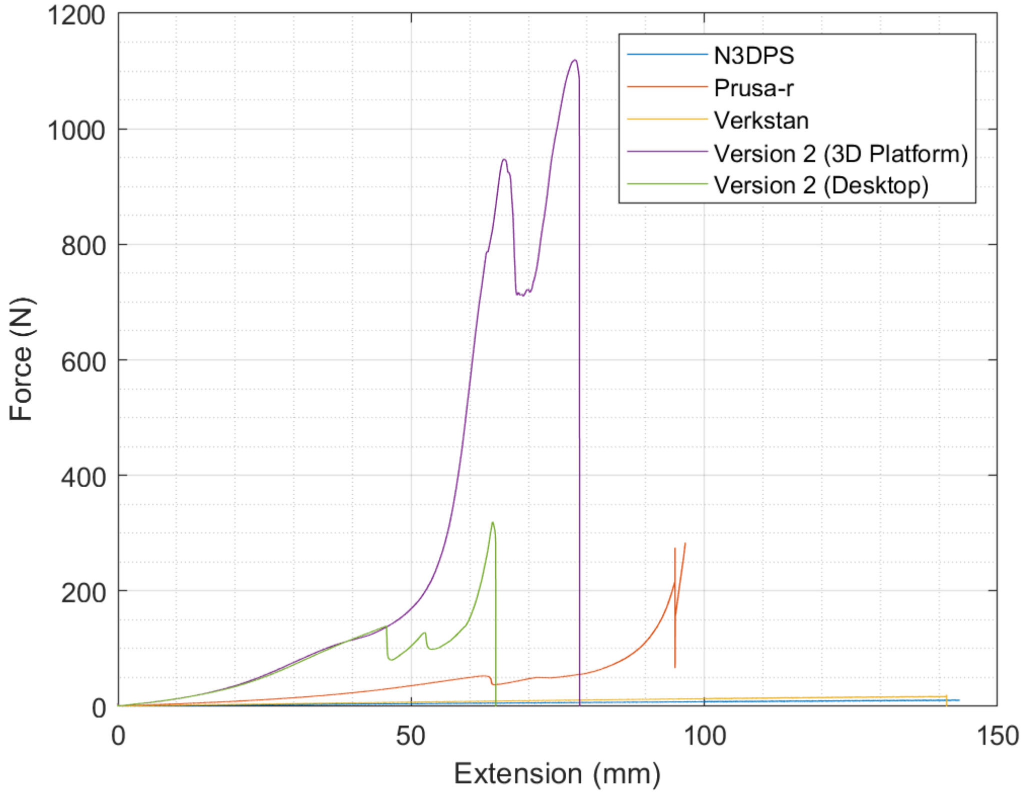

Figure 6: Mechanical testing results of the 3D Printed headbands.

4. Conclusions

LSAM has been shown to be a technology capable of producing components of PPE devices in significantly less time than the traditional 3D printing systems such as desktop FFF devices. Through the thorough understanding of the interplay between design and process parameters, it is feasible to parametrically optimising a design for a simple thermoplastic component for production using LSAM, with areas of the design that would typically take a number of nozzles passes with a traditional sub-mm nozzle able to be deposited with just a single pass from a nozzle on a LSAM system. By leveraging the key advantages of LSAM it is possible to achieve production rates up to 20× faster than traditional desktop 3D printing, achieving a production rate that more closely bridges to manufacturing processes such as injection moulding.

4. Acknowledgements

The authors would like to acknowledge 3DFilaPrint Ltd for support with the sourcing and provision of material for the project and the EPSRC for the PhD studentship for EGB.

5. Conflict of Interest

No conflict of interest was reported by all authors

6. References

[1] J. Riou and C. L. Althaus, "Pattern of early human-to-human transmission of Wuhan 2019 novel coronavirus (2019-nCoV), December 2019 to January 2020," *Euro Surveill,* vol. 25, no. 4, Jan 2020, doi: 10.2807/1560-7917.ES.2020.25.4.2000058.

[2] C. I. Paules, H. D. Marston, and A. S. Fauci, "Coronavirus Infections-More Than Just the Common Cold," *JAMA,* Jan 23 2020, doi: 10.1001/jama.2020.0757.

[3] Q. Li, X. Guan, P. Wu, X. Wang, L. Zhou, Y. Tong, R. Ren, K.S. Leung, E.H. Lau, J.Y. Wong and X. Xing "Early Transmission Dynamics in Wuhan, China, of Novel Coronavirus-Infected Pneumonia," *N Engl J Med,* vol. 382, no. 13, pp. 1199-1207, Mar 26 2020, doi: 10.1056/NEJMoa2001316.

[4] World Health Organization, "WHO Virtual Press Conference on COVID-19," 2020. [Online]. Available: https://www.who.int/docs/default-source/coronaviruse/transcripts/who-audio-emergencies-coronavirus-press-conference-22apr2020.pdf?sfvrsn=4f8821b6_2.

[5] World Health Organisation, "Coronavirus disease 2019 (COVID-19): situation report, 112.," 2020.

[6] Y. Liu, A. A. Gayle, A. Wilder-Smith, and J. Rocklov, "The reproductive number of COVID-19 is higher compared to SARS coronavirus," *J Travel Med,* vol. 27, no. 2, Mar 13 2020, doi: 10.1093/jtm/taaa021.

[7] A. Ather, B. Patel, N. B. Ruparel, A. Diogenes, and K. M. Hargreaves, "Coronavirus Disease 19 (COVID-19): Implications for Clinical Dental Care," *J Endod,* vol. 46, no. 5, pp. 584-595, May 2020, doi: 10.1016/j.joen.2020.03.008.

[8] Y. Bai, L. Yao, T. Wei, F. Tian, D.Y. Jin, L. Chen and M. Wang, "Presumed Asymptomatic Carrier Transmission of COVID-19," *JAMA,* Feb 21 2020, doi: 10.1001/jama.2020.2565.

[9] World Health Organization, "Rational use of personal protective equipment for coronavirus disease 2019 (COVID-19)," 2020.

[10] World Health Organization, "Modes of transmission of virus causing COVID-19: implications for IPC precaution recommendations," *Intensive Care Med,* vol. 46, no. 5, pp. 854-887, May 2020, doi: 10.1007/s00134-020-06022-5.

[11] E. Livingston, A. Desai, and M. Berkwits, "Sourcing personal protective equipment during the COVID-19 pandemic.," *JAMA,* 2020.

[12] E. Larrañeta, J. Dominguez-Robles, and D. A. Lamprou, "Additive Manufacturing Can Assist in the Fight Against COVID-19 and Other Pandemics and Impact on the Global Supply Chain," *3D Printing and Additive Manufacturing,* 2020, doi: 10.1089/3dp.2020.0106.

[13] S. T. Flanagan and D. H. Ballard, "3D Printed Face Shields: A Community Response to the COVID-19 Global Pandemic," *Acad Radiol,* Apr 17 2020, doi: 10.1016/j.acra.2020.04.020.

[14] W. Phillips *et al.*, "Redistributed Manufacturing in Healthcare: Creating New Value through Disruptive Innovation," 2017, doi: 10.13140/RG.2.2.11461.14567.

[15] H. Tardieu, D. Daly, J. Esteban-Lauzán, J. Hall, and G. Miller, "Case Study 6: The digital Transformation of Manufacturing," in *Deliberately Digital*: Springer, 2020, pp. 269-280.

[16] B. Redwood, F. Schöffer, and B. Garret, *The 3D Printing Handbook*. 2017.

[17] E3D Blog, E3D, [Online]. Available: https://e3d-online.com/blog/2019/02/28/supervolcano/. viewed May 13, 2020

[18] B. K. Post, P.C Chesser, R.F. Lind, A. Roschli, L.J. Love, K.T. Gaul, M. Sallas, F. Blue and S. Wu, "Using Big Area Additive Manufacturing to directly manufacture a boat hull mould," *Virtual and Physical Prototyping*, vol. 14, no. 2, pp. 123-129, 2018, doi: 10.1080/17452759.2018.1532798.

[19] V. Kunc, A. A. Hassen, J. Lindahl, S. Kim, B. Post, and L. Love, "LARGE SCALE ADDITIVELY MANUFACTURED TOOLING FOR COMPOSITES," 2017.

[20] B. K. Post, B. Richardson, R. Lind, L. J. Love, P. Lloyd, V. Kunc, B. J. Rhyne, A. Roschli, J. Hannan, S. Nolet, K. Veloso, P. Kurup, T. Remo, and D. Jenne, “BIG AREA ADDITIVE MANUFACTURING APPLICATION IN WIND TURBINE MOLDS," in Solid Freeform Fabrication 2017: Proceedings of the 28th Annual International Solid Freeform Fabrication Symposium, 2017.

[21] D. Moreno Nieto, V. Casal López, and S. I. Molina, "Large-format polymeric pellet-based additive manufacturing for the naval industry," *Additive Manufacturing*, vol. 23, pp. 79-85, 2018, doi: 10.1016/j.addma.2018.07.012.

[22] A. Murat, "Additive Manufacturing: Is It a New Era for Furniture Production?," *Journal of Mechanics Engineering and Automation*, vol. 5, no. 6, 2015, doi: 10.17265/2159-5275/2015.06.002.

[23] "Continuous CF bike frame," *Reinforced Plastics*, vol. 63, no. 4, 2019, doi: 10.1016/j.repl.2019.06.043.

[24] National 3D Printing Society. "Medical AM (COVID-19)." https://national3dprintingsociety.co.uk/medical-am-covid-19/ (viewed 1 June, 2020).

[25] Prusa Research. "Prusa Face Shield." https://www.prusaprinters.org/prints/25857-prusa-face-shield (viewed 1 June, 2020).

[26] 3DVerkstan. "3D-PRINTED PROTECTIVE VISOR." https://3dverkstan.se/protective-visor/ (viewed 1 June, 2020).

[27] R. Devicharan and R. Garg, "Optimization of the Print Quality by Controlling the Process Parameters on 3D Printing Machine," in *3D Printing and Additive Manufacturing Technologies* Singapore: Springer, 2019, pp. 187-194.

[28] M. Galatia *et al.*, "A methodology for evaluating the aesthetic quality of 3D printed part," *Procedia CIRP*, vol. 79, no. 1, pp. 95-100, 2019.